



Cite this: *Chem. Commun.*, 2018, 54, 7306

Received 27th March 2018,
Accepted 21st May 2018

DOI: 10.1039/c8cc02483a

rsc.li/chemcomm

A generalized approach for NMR studies of lipid–protein interactions based on sparse fluorination of acyl chains†

Alfredo De Biasio,^{‡§*} Alain Ibáñez de Opakua,[§] Mark J. Bostock,^{‡b} Daniel Nietlispach,^{‡b} Tammo Diercks^{‡b*} and Francisco J. Blanco^{‡b*ac}

Sparse lipid fluorination enhances the lipids' ¹H signal dispersion, enables clean molecular distinction by ¹⁹F NMR, and evinces micelle insertion of proteins via fluorine-induced signal shifts. We present a minimal fluorination scheme, and illustrate the concept on di-(4-fluoro)-heptanoylphosphatidylcholine micelles and solubilised seven-helix transmembrane pSRII protein.

Lipid–protein interactions within cell membranes remain poorly characterized despite high relevance in physiological and pathological processes. Bound lipid molecules are rarely visible in the known membrane protein structures as the conformational heterogeneity and dynamics in lipid layers impede their orderly crystallisation for X-ray¹ or fine classification for cryo-EM² studies. In contrast, NMR spectroscopy does not require molecular order and generic lipid–protein contacts may be sampled more coarsely to gauge protein insertion into the lipid layer, *e.g.* by use of paramagnetic agents.³ High resolution analyses of lipid–protein contacts require more range-limited, directed, and unambiguous NMR indicators. Ultimately, specific lipid–protein contacts are revealed by intermolecular ¹H, ¹H NOE signals,⁴ but their identification and resolution are impeded by the generally poor ¹H signal dispersion in lipid acyl chains. The classic workaround to correlate ¹H with ¹³C frequencies is impractical for lipids, where ¹³C isotope enrichment may not resolve all overlap problems and provides no distinct molecular marker from a likewise ¹³C labelled protein to single out inter- from intramolecular NOEs.

We propose an approach for NMR studies of lipid–protein interactions that relies on sparse fluorination of the lipid acyl chains and exploits fluorine both indirectly, as a shift reagent affecting nearby NMR spins, and directly, as ¹⁹F isotope with unique NMR properties. The introduced fluorine atoms then solve the NMR resolution problem for acyl chains by (i) increasing their ¹H signal dispersion *via* local deshielding, (ii) enabling clean molecular distinction *via* ¹⁹F filtering, and (iii) allowing further resolution enhancement *via* ¹⁹F editing. Fluorine may also induce chemical shift perturbation (CSP) in nearby protein spins to indicate protein insertion into lipid layers similar to paramagnetic markers, but with minimal steric impact. In this introductory study we focus on the indirect NMR effects of fluorine and demonstrate its utility as both intra- and intermolecular shift reagent. We derive a minimal fluorination scheme for acyl chains and show that a single hydrogen-to-fluorine substitution induces a fully resolved ¹H spectrum for 4F-DHPC₇ without impairing micelle formation or stabilisation of the phototaxis receptor sensory rhodopsin II (pSRII). The H/F substitution in the lipid provokes CSP for amide groups near both ends of the seven-helix bundle, elucidating its micelle insertion.

¹⁹F NMR studies on partially fluorinated membrane proteins have already yielded information on their structure in membrane mimicking environments.^{5,6} Complementary studies on fluorinated lipids focused on analyzing lipid phase properties.^{7–10} Use of fluorinated lipids and ¹⁹F NMR to investigate protein–lipid interactions was suggested before,¹¹ but not explored presumably for technical deficiencies with regard to (i) preparing the required quantities of membrane protein with isotope enrichment and reconstituted in micelles or bicelles; (ii) synthesizing sparsely fluorinated lipids; and (iii) NMR methodology and hardware. Advances in these fields¹² now make it possible to develop the experimental approach delineated here.

Replacing hydrogen by fluorine is a chemical modification that may affect the lipid's biophysical properties and interaction with membrane proteins. It also reduces the ¹H density and, thus, coverage of (fluoro)lipid–protein contacts *via* ¹H, ¹H NOE signals.

^a CIC bioGUNE, Derio, Spain. E-mail: tdiercks@cicbiogune.es, fblanco@cicbiogune.es

^b Department of Biochemistry, University of Cambridge, Cambridge, UK

^c IKERBASQUE, Basque Foundation for Science, Bilbao, Spain

† Electronic supplementary information (ESI) available: Experimental procedures, figures and tables. See DOI: 10.1039/c8cc02483a

‡ Present address: Department of Molecular and Cell Biology, Leicester Institute of Structural and Chemical Biology, University of Leicester, Leicester, UK. E-mail: adb43@leicester.ac.uk

§ These authors contributed equally.



Hence, the number of H/F substitutions must be minimized, but still ensure enough fluorine induced deshielding to separate all acyl chain ^1H signals. Its reach may be deduced from the spectrum of 1-palmitoyl-2-(16-fluoropalmitoyl)phosphatidylcholine¹³ with one terminal fluorine on acyl chain 2 (Avanti Polar Lipids). Comparison of ^1H , ^1H -TOCSY traces of both chains (Fig. S1, ESI†) reveals that the single H/F substitution shifts the geminal ^1H by *ca.* +3.5 ppm, vicinal ^1H by +0.35 ppm, and the ^1H four bonds away by +0.09 ppm. Also, heteronuclear J_{HF} coupling is strong to geminal ($^2J_{\text{HF}} \approx 50$ Hz) and vicinal ^1H ($^3J_{\text{HF}} \approx 10\text{--}35$ Hz), and still notable over four bonds ($^4J_{\text{HF}} < 10$ Hz). The induced ^1H deshielding over ± 2 carbon positions stipulates optimal fluorine spacing by 5 positions. Even unmodified acyl chains show resolved signals for the ^1H bound to C2 (>2.0 ppm), C3 (>1.5 ppm), and the terminal C ω (<1.0 ppm), while those bound from C4 to C $\omega - 1$ overlap at 1.4 ± 0.1 ppm. Acyl chains with $z_{\text{C}} > 5$ carbon atoms, thus, require ^1H dispersion enhancement by single H/F substitution at carbon atoms $i \pm m \cdot 5$, starting ≤ 3 positions from the first (C3) or last (C ω) resolved CH_n group, *i.e.* at positions $i \leq 6$ or $i \geq \omega - 3$. This minimal fluorination scheme (Fig. 1) implies introduction of $z_{\text{F}} \leq z_{\text{C}}/5$ fluorine atoms (rounded down), leaving $z_{\text{H}} = 2 \cdot z_{\text{C}} - 1 - z_{\text{F}}$ protons. Thus, less than 11% of all acyl chain protons need to be exchanged for fluorine.

Our transmembrane test protein pSRII¹⁴ is best stabilized in diheptanoylphosphatidylcholine (DHPC₇) micelles, where the minimal fluorination scheme suggests H/F substitution at C4 or C5. Opting for the former, we obtained di-(4-fluoro)heptanoylphosphatidylcholine (4F-DHPC₇) by custom synthesis (Avanti Polar Lipids). NMR diffusion measurements proved stable micelle formation up to at least 323 K (Fig. S2, ESI†). A CMC of 12.7 mM was derived from the concentration dependence of diffusion coefficients¹⁵ (Fig. 2), about sevenfold higher than for unfluorinated DHPC₇ (1.7 mM) but similar to DHPC₆ (14 mM).¹⁵ The also derived hydrodynamic micelle radii, r_{m} , of some 29 Å for 4F-DHPC₇ and 34 Å for DHPC₇ may suggest smaller micelles for 4F-DHPC₇, but still agree within errors.

The acyl chain ^1H NMR spectrum in the micelle (Fig. 3) shows the typical degeneracy of the central H4 to H6 protons for DHPC₇, but full dispersion for 4F-DHPC₇ induced by the fluorine atom. Even the diastereotopic H3, H5, and H6 methylene protons

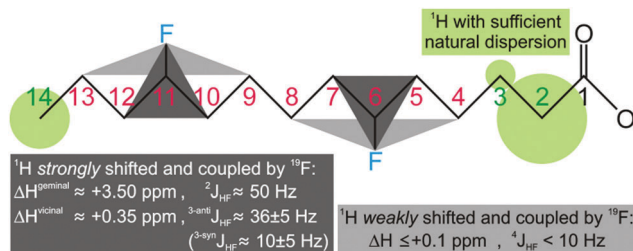


Fig. 1 Minimal fluorination scheme for acyl chains, shown for the myristoyl group (C₁₄). The reach of fluorine induced ^1H deshielding (and heteronuclear $^nJ_{\text{HF}}$ coupling) suggests single H/F substitution at carbon atoms $i \pm m \cdot 5$, where the natural H2, H3, and H ω signal dispersion sets the start position i to ≤ 6 or $\geq \omega - 3$ (with $m = 0, 1, 2, \dots, z_{\text{F}} - 1$).

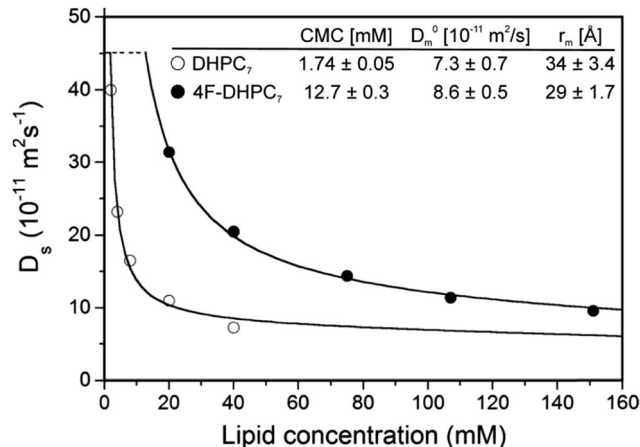


Fig. 2 Diffusion coefficients for DHPC₇ (○) and 4F-DHPC₇ (●) as a function of the lipid concentration, obtained at 298 K from the most intense ^1H and ^{19}F NMR signal, respectively. Derived critical micelle concentration, CMC, diffusion coefficient at infinite dilution, D_m^0 , and hydrodynamic radius, r_m , are indicated.

are resolved, and larger (36 ± 5 Hz) or smaller (10 ± 5 Hz) $^3J_{\text{HF}}$ coupling constants identify the H3 and H5 protons in *anti*- or *syn*-clinal position to the F4 atom, respectively. The latter enables further editing in a ^{19}F dimension, where correlation with all acyl ^1H signals is achieved in a 2D ^1H , ^{19}F TOCSY-COLOC¹⁶ spectrum (Fig. 3). Remarkably, the ^{19}F spectrum of 4F-DHPC₇ shows six distinct signals, with double integral for both downfield signals that correlate with also downfield shifted H2 to H4 signals. H2 correlation with glycerol C1' or C2' by long-range ^{13}C HSQC then assigns the four upfield ^{19}F signals to acyl chain 1 and both degenerate downfield ^{19}F signals to chain 2. The distinct ^{19}F signals most likely arise from the four stereoisomers of 4F-DHPC₇ with its 3 chiral carbon atoms, where the *sn*2-glycerol C2' has fixed *R* configuration while H/F substitution at both acyl chain C4 was not stereospecific. Only the acyl ^{13}C O signals show dispersion similar to ^{19}F and have higher shifts for chain 1, contrary to higher shifted ^{19}F , ^1H , and aliphatic ^{13}C signals in chain 2. Table S1 (ESI†) lists the complete assignment for 4F-DHPC₇ micelles.

We next verified that 4F-DHPC₇ micelles can stabilize pSRII as efficiently as DHPC₇ for high resolution NMR studies.¹⁴ Overall similar TROSY spectra of pSRII in 4F-DHPC₇ and DHPC₇ micelles (Fig. 4) indicate matching protein structures, but some amide signals differ more clearly. After reassigning 194 signals (84% of expected 230 signals, *cf.* Table S2, ESI†) we quantified their CSP caused by the H/F substitution in 4F-DHPC₇ (Fig. 4, below). 26 residues show significant CSP larger than the average of all 194 CSP values ($\phi_{\text{CSP}} = 0.023$ ppm) plus their standard deviation ($\sigma_{\text{CSP}} = 0.019$ ppm), including 6 residues with a CSP $> \phi_{\text{CSP}} + 2 \cdot \sigma_{\text{CSP}}$. These residues cluster within two bands near both ends of the transmembrane seven-helix bundle and indicate proximity to the fluorine atoms in 4F-DHPC₇, thus guiding the sketched alignment of lipid molecules adjacent to embedded pSRII (Fig. 5). The picture for micelle insertion emerging from fluorine induced CSP mapping agrees in detail with that from paramagnetic relaxation enhancement:¹⁴ pSRII inserts asymmetrically into the micelle, while the rather large



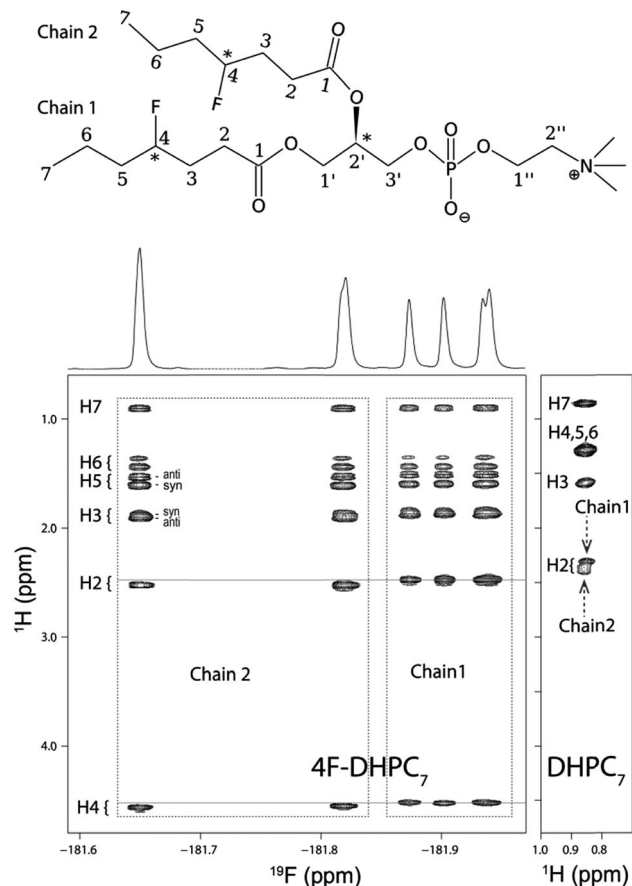


Fig. 3 (top) 4F-DHPC₇ with carbon atoms numbered for the acyl, glycerol ('), and choline (") moieties. Three chiral centres (*) give rise to 2² stereoisomers since the *R* configuration at C2' is fixed. (below) 2D ¹H, ¹⁹F TOCSY-COLOC spectrum of 4F-DHPC₇ acyl chains in micelles (298 K, 600 MHz). All ¹H signals are resolved, also the diastereotopic H3, H5, and H6 signals (indicated *syn/anti* positions relate to the fluorine atom); the H2 to H4 shifts differ slightly for both acyl chains. The ¹⁹F spectrum (projected above) separates both acyl chains and stereoisomers. (below, right) 2D TOCSY spectrum of DHPC₇ micelles (H7 strip) showing the poor ¹H signal dispersion typical for unmodified acyl chains, where only H2, H3, and the terminal H7 are resolved.

gap (ca. 10 Å) between opposed 4F-DHPC₇ molecules allows for the suggested tail-on filling by further lipid molecules according to a prolate micelle model. This agreement validates fluorine induced CSP as an alternative indicator for lipid layer insertion. In contrast to bulky paramagnetic markers, fluorine may be inserted anywhere along the acyl chain, thus allowing to probe lipid layer insertion stepwise and with more precision owing to the shorter reach of fluorine induced CSP.

Besides deshielding through space, fluorine induced CSP might conceivably also derive from local rearrangements in the protein. Yet these should not be significant since even the major CSP amplitudes remain too small and mostly localise on amide groups forming part of well defined secondary structure in pSRII. There, any larger conformational changes would impair the stabilising hydrogen bond network and levy a high energetic penalty, which should also affect local dynamics and NMR relaxation rates. Yet the ratios of pSRII amide signal

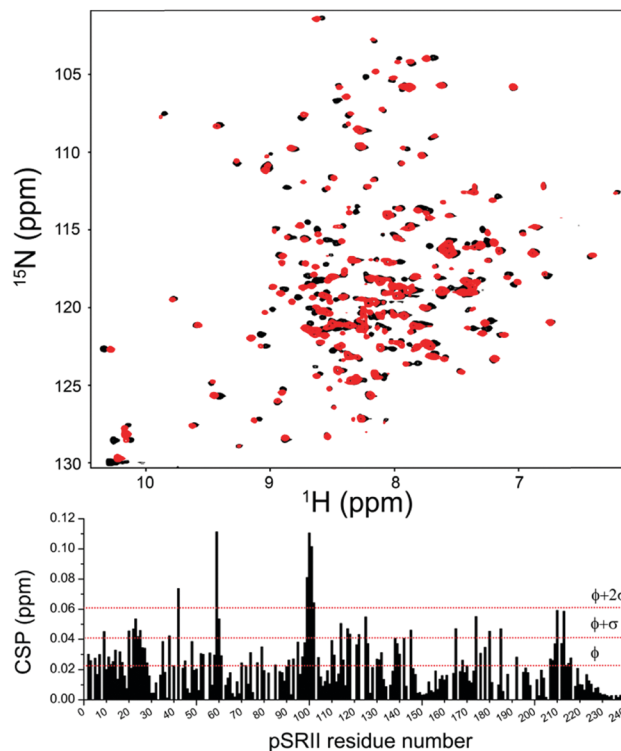


Fig. 4 (top) 2D ¹H, ¹⁵N TROSY spectrum of pSRII in DHPC₇ (black) or 4F-DHPC₇ (red) micelles (32 mM lipid, 50 mM sodium phosphate pH 5.9, 50 mM NaCl, 308 K, 800 MHz). (below) Chemical shift perturbation, CSP, versus amino acid number, derived from ¹⁵N and ¹H_N shift differences between both media. Horizontal red lines indicate the average CSP (ϕ) plus one or two standard deviations (σ), computed over all 194 reassigned signals.

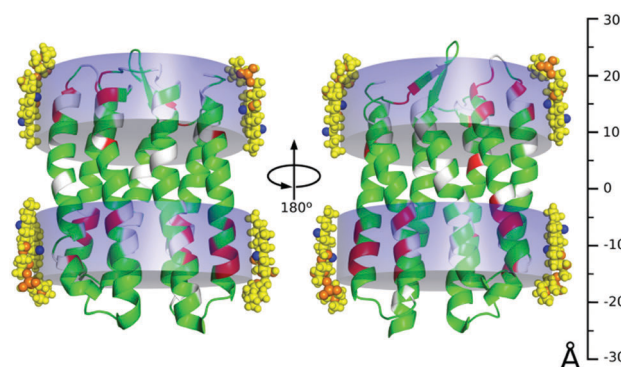


Fig. 5 Model of pSRII (PDB 2KSY) insertion into 4F-DHPC₇ micelles. Residues with a fluorine induced amide CSP above (red; below = green) the average plus one standard deviation cluster near both ends of the seven-helix bundle (unassigned residues in grey; the omitted disordered C-terminal residues 222–241 show no significant CSP). 4F-DHPC₇ molecules were modeled adjacent to pSRII by aligning their fluorine atoms (blue; orange = oxygen, phosphorus, nitrogen) with the bands of induced CSP (transparent blue). The scale on the right is centered with the seven-helix bundle to underscore the indicated asymmetric micelle insertion of pSRII, where helices protrude farther on the cytosolic side (at the bottom).

intensities in 4F-DHPC₇ versus DHPC₇ micelles, which relate to their net *T*₂ relaxation times, clearly do not correlate with the CSP values (Fig. S3, ESI[†]). Normalised pSRII signal intensities



nevertheless appear to be *ca.* 10% lower on average in 4F-DHPC₇ micelles, possibly due to some line broadening from more lipid exchange with the solution, as indicated by the higher CMC.

A next step along the proposed approach would be to explore the possibilities for ¹⁹F NMR enabled by the sparsely fluorinated lipids, where the main challenge is efficient inphase correlation of all acyl chain ¹H with the sparse ¹⁹F spins for global selection by ¹⁹F filtering. This then allows implementation of diagonal-free ¹H[¹⁹F], ¹H[¹³C/¹⁵N] NOESY experiments with orthogonal isotope filtering for ¹⁹F (on the acyl chain) *versus* ¹³C or ¹⁵N bound protons (on the protein) to only observe intermolecular lipid–protein contacts. While complete ¹H, ¹⁹F correlation was obtained with the ¹H, ¹⁹F TOCSY-COLOC¹⁶ experiment (Fig. 3), ¹H, ¹⁹F Hetero-TOCSY mixing¹⁷ would achieve more efficient, robust, and directly inphase heteronuclear transfer with accompanying homonuclear ¹H, ¹H TOCSY transfer that is generally needed for correlation beyond the reach of heteronuclear ⁿJ_{HF} coupling. Implementation, however, requires special NMR hardware (*i.e.* two high-frequency amplifiers for simultaneous ¹H and ¹⁹F pulsing). The envisaged diagonal-free ¹H[¹⁹F], ¹H[¹³C/¹⁵N] NOESY experiment to selectively observe lipid–protein contacts then derives from a standard NOESY-(¹³C/¹⁵N)HSQC by prepending the NOESY with a heteronuclear ¹⁹F, ¹H TOCSY transfer step. This concatenation corresponds to the ³¹P, ¹H Hetero-TOCSY-NOESY experiment¹⁸ that was successfully used for efficient RNA assignment. The ¹⁹F, ¹H analogue should be an order of magnitude more sensitive owing to the much larger heteronuclear couplings (ⁿJ_{HF} ≤ 50 Hz *vs.* ⁿJ_{HP} < 12 Hz) and polarisation ($\gamma_F/\gamma_P \approx 2.3$) exploited.

The lipid chosen for this introductory study forms micelles that may not be the most appropriate membrane mimics. Nevertheless, two key results of this study have general validity: properly selected sparse fluorination of acyl chains greatly enhances their ¹H signal dispersion, and also causes notable CSP in membrane proteins that gauge their insertion into the lipid phase. Other sparsely fluorinated lipids forming more membrane-like phases, such as nanodiscs,¹⁹ may next be tested to establish the generality of the proposed approach. The primary challenges expected for these larger, more asymmetric lipid systems arise from possibly faster ¹⁹F T₂ relaxation.

Yet while this would compromise ¹⁹F editing, ¹⁹F filtering may still be implemented with minimal sensitivity to T₂ relaxation.

We thank MINECO for the Severo Ochoa Excellence Accreditation (SEV-2016-0644) and for the grant CTQ2017-83810-R to FJB. We dedicate this communication to the memory of Chris Spronk.

Conflicts of interest

There are no conflicts to declare.

References

- 1 S. H. White, A. S. Ladokhin, S. Jayasinghe and K. Hristova, *J. Biol. Chem.*, 2001, **276**, 32395–32398.
- 2 S. Rawson, S. Davies, J. D. Lippiat and S. P. Muench, *Mol. Membr. Biol.*, 2016, **33**, 12–22.
- 3 R. S. Prosser, F. Evanics, J. L. Kitevski and S. Patel, *Biochim. Biophys. Acta*, 2007, **1768**, 3044–3051.
- 4 C. Fernandez, C. Hilty, G. Wider and K. Wuthrich, *Proc. Natl. Acad. Sci. U. S. A.*, 2002, **99**, 13533–13537.
- 5 J. L. Kitevski-LeBlanc and R. S. Prosser, *Prog. Nucl. Magn. Reson. Spectrosc.*, 2012, **62**, 1–33.
- 6 T. Didenko, J. J. Liu, R. Horst, R. C. Stevens and K. Wuthrich, *Curr. Opin. Struct. Biol.*, 2013, **23**, 740–747.
- 7 J. M. Sturtevant, C. Ho and A. Reimann, *Proc. Natl. Acad. Sci. U. S. A.*, 1979, **76**, 2239–2243.
- 8 B. McDonough, P. M. Macdonald, B. D. Sykes and R. N. McElhaney, *Biochemistry*, 1983, **22**, 5097–5103.
- 9 P. M. Macdonald, B. D. Sykes and R. N. McElhaney, *Biochemistry*, 1985, **24**, 4651–4659.
- 10 Z. Y. Peng, N. Tjandra, V. Simplaceanu and C. Ho, *Biophys. J.*, 1989, **56**, 877–885.
- 11 E. A. Pratt, J. A. Jones, P. F. Cottam, S. R. Dowd and C. Ho, *Biochim. Biophys. Acta*, 1983, **729**, 167–175.
- 12 J. Guimond-Tremblay, M. C. Gagnon, J. A. Pineault-Maltais, V. Turcotte, M. Auger and J. F. Paquin, *Org. Biomol. Chem.*, 2012, **10**, 1145–1148.
- 13 D. J. Hirsh, N. Lazaro, L. R. Wright, J. M. Boggs, T. J. McIntosh, J. Schaefer and J. Blazyk, *Biophys. J.*, 1998, **75**, 1858–1868.
- 14 A. Gautier, H. R. Mott, M. J. Bostock, J. P. Kirkpatrick and D. Nietlispach, *Nat. Struct. Mol. Biol.*, 2010, **17**, 768–774.
- 15 J. J. Chou, J. L. Baber and A. Bax, *J. Biomol. NMR*, 2004, **29**, 299–308.
- 16 T. M. O'Connell and R. E. London, *J. Magn. Reson., Ser. B*, 1995, **109**, 264–269.
- 17 H. Hu, P. Kulanthaivel and K. Krishnamurthy, *J. Org. Chem.*, 2007, **72**, 6259–6262.
- 18 G. W. Kellogg, A. A. Szewczak and P. B. Moore, *J. Am. Chem. Soc.*, 1992, **114**, 2727–2728.
- 19 R. Puthenveetil, K. Nguyen and O. Vinogradova, *Nanotechnol. Rev.*, 2017, **6**, 111–126.

